International Journal of Engineering, Mathematical and Physical Sciences
ISSN: 2517-9934
Vol:10, No:9, 2016

FEM Simulation of Triple Diffusive Magnetohydrodynamics Effect of Nanofluid Flow over a Nonlinear Stretching Sheet

Rangoli Goyal, Rama Bhargava

***Abstract*—**The triple diffusive boundary layer flow of nanofluid under the action of constant magnetic field over a non-linear stretching sheet has been investigated numerically. The model includes the effect of Brownian motion, thermophoresis, and cross-diffusion; slip mechanisms which are primarily responsible for the enhancement of the convective features of nanofluid. The governing partial differential equations are transformed into a system of ordinary differential equations (by using group theory transformations) and solved numerically by using variational finite element method. The effects of various controlling parameters, such as the magnetic influence number, thermophoresis parameter, Brownian motion parameter, modified Dufour parameter, and Dufour solutal Lewis number, on the fluid flow as well as on heat and mass transfer coefficients (both of solute and nanofluid) are presented graphically and discussed quantitatively. The present study has industrial applications in aerodynamic extrusion of plastic sheets, coating and suspensions, melt spinning, hot rolling, wire drawing, glass-fibre production, and manufacture of polymer and rubber sheets, where the quality of the desired product depends on the stretching rate as well as external field including magnetic effects.

***Keywords*—**FEM, Thermophoresis, Diffusiophoresis, Brownian motion.

I. Introduction

THERMAL properties of liquids play a decisive role in heating as well as cooling applications in industrial processes. Commonly used heat transfer fluids such as water, ethylene glycol, toluene, or oil have inherently poor thermal conductivity which makes them inadequate for ultra-high cooling applications. A recent technique to improve the thermal conductivity of these fluids is to introduce nanosized metallic particles such as aluminum, iron, gold, copper, or their oxides, and carbides in the fluids by suspension.

Masuda et. al. [19] and Choi et.al. [20] have affirmed that the addition of a very small amount of nanoparticles (usually below 5%) can provide remarkable improvement in thermal conductivity and heat transfer coefficient as compared to the base fluid. The term nanofluids was proposed by Choi and Eastman [21] to describe this new class of nanotechnology–based heat transfer fluids that exhibit thermal properties superior to those of their base fluids or traditional particle fluid suspensions. A comprehensive study of convective transport in nanofluids was made by Buongiorno [2]. He discussed the reasons of heat transfer enhancement for nanofluids and concluded that Brownian diffusion and thermophoresis are two important nanoparticle/base-fluid slip mechanisms. The flow over a stretching sheet has important engineering applications, especially in the field of metallurgy and chemical engineering processes that involve cooling of continuous strip or filament by drawing them through a dormant fluid. Sakiadis [16] initiated a study in stretching sheet by investigating the boundary layer flow due to a sheet issuing with constant speed from a slit into a fluid at rest. An extension to this problem was made by Crane [22]. After this pioneering work, analysis of flow, and heat transfer over a stretching surface has drawn considerable attention and have been studied in recent years [1], [8]-[10]. All the above mentioned studies were performed by taking into account either a constant value for the velocity wall or a linearly stretching sheet problem (i.e., $u_w(x)= ax$). However, the stretching of the sheet may not necessarily be linear. With this idea in mind, flow over a non-linear stretching sheet was analysed by many researchers. Vajravelu [17] numerically discussed the viscous flow over a stretching sheet moving with nonlinear velocity (i.e., $u_w(x)=ax^n$). He computed numerical solutions for various values of power law index n. Cortell [3] extended this model by considering two different types of thermal boundary conditions on the sheet, constant surface temperature, and prescribed surface temperature. Kumaran and Ramaniah [8] studied the boundary layer fluid flow where, the stretching sheet is assumed to be quadratic. Kechil and Hashim [6] derived analytic solutions for MHD flow over a non-linear stretching sheet by Adomian decomposition method. Hamad et. al. [5] provided the similarity solutions to flow and heat transfer of nanofluid over non-linear stretching surface. Ziabakhsh et al. [23] studied the impact of chemical reaction on the flow over a non-linear stretching sheet embedded in porous medium. Narayana et al. [12] and Vajravelu et al. [18] studied the nanofluid flow over a nonlinear stretching sheet. Goyal and Bhargava [4] studied the thermodiffusion effects on boundary layer flow of nanofluids over a power law stretching sheet. In such problems, magnetohydrodynamics (MHD) effects are considered important since these allow for control of the rate of cooling in order to achieve a final product with the desired characteristics as well as the separation of molten metals from non-metallic impurities. The MHD flow over a moving plate is of interest due to its increasing importance in a great deal of processing

Rangoli Goyal is with Indian Institute of Technology Roorkee, Roorkee – 247667, Uttarakhand, India (Phone: 01332-285039, e-mail: rangoligoyal@gmail.com).

Rama Bhargava is with Indian Institute of Technology Roorkee, Roorkee – 247667, Uttarakhand, India (e-mail: rbharfma@iitr.ac.in).

industries such as petroleum engineering, metallurgy industry, chemical engineering, and so on. Researchers have studied the MHD effects on fluid flow in the past [11], [13], [14].

Inspired by the above investigations, authors contemplate to study the heat and mass transfer for the flow of nanofluid over a non-linear stretching sheet with thermodiffusion effects under constant magnetic field. To the best of our knowledge, FEM simulation of this problem has not been done so far.

II. Mathematical Analysis

A steady state two dimensional natural convection boundary layer flow of Al_2O_3-water nanofluid on a nonlinear stretching sheet with variable magnetic field is considered.

The sheet is saturated in a medium which is a binary fluid with dissolved solutal and containing nanoparticles in suspension. The nanoparticle concentration by volume is 0.04. The nanoparticles and fluid phase are assumed to be in thermal equilibrium state. The x-axis is assumed to be in the direction of the flow and the y-axis to be perpendicular to it. The x-axis is taken to be in horizontal direction. The plate is considered at y=0. In its plane, the sheet is stretched with the velocity $U= u_w(x)=ax^m$ (where m is the nonlinear stretching parameter, a>0 is the constant acceleration parameter). The temperature at the sheet (T_w) is larger than the ambient temperature (T_∞). The pressure gradient and external forces are neglected.

For incompressible fluid flow, with the boundary layer approximation, the field equations as derived by Buongiorno [2] and Khan et. al. [7] representing conservation of mass, momentum, thermal, solute, and nanoparticles, can be written as

$$\frac{\partial u}{\partial x}+\frac{\partial v}{\partial y}=0 \tag{1}$$

$$u\frac{\partial u}{\partial x}+v\frac{\partial u}{\partial y}=\upsilon\frac{\partial^2 u}{\partial y^2}-\frac{\sigma B_o^2}{\rho}u \tag{2}$$

$$u\frac{\partial T}{\partial x}+v\frac{\partial T}{\partial y}=\alpha_m\frac{\partial^2 T}{\partial y^2}+\tau\left\{D_B\frac{\partial \phi}{\partial y}\frac{\partial T}{\partial y}+\frac{D_T}{T_\infty}\left(\frac{\partial T}{\partial y}\right)^2\right\}+D_{TC}\frac{\partial^2 C}{\partial y^2} \tag{3}$$

$$u\frac{\partial C}{\partial x}+v\frac{\partial C}{\partial y}=D_S\frac{\partial^2 C}{\partial y^2}+D_{CT}\frac{\partial^2 T}{\partial y^2} \tag{4}$$

$$u\frac{\partial \phi}{\partial x}+v\frac{\partial \phi}{\partial y}=D_B\frac{\partial^2 \phi}{\partial y^2}+\frac{D_T}{T_\infty}\frac{\partial^2 T}{\partial y^2} \tag{5}$$

The boundary conditions for the velocity, temperature, and concentration fields are given as follows:

$$\begin{aligned} &u=u_w(x), v=0, T=T_w(x), C=C_w(x), \phi=\phi_w(x) \ at\ y=0 \\ &u=0, T=T_\infty, C=C_\infty, \phi=\phi_\infty \ as\ y\to\infty \end{aligned} \tag{6}$$

where the subscripts w and ∞ indicate the conditions at the wall and at the outer edge of the boundary layer, respectively.

(u,v) are the velocity components in (x, y) directions, ρ_f is the density of base fluid, ρ_p is the nanoparticle density, μ is the dynamic viscosity of the base fluid, ν is the kinematic viscosity of the base fluid, σ is the electrical conductivity of the base fluid, B_0 is the strength of magnetic field, T is the fluid temperature, α_m is the thermal diffusivity, $\tau\ (=(\rho C)_p\ /\ (\rho C)_f)$ is the ratio of effective heat capacity of the nanoparticle material to heat capacity of the fluid, is the nanoparticle volume fraction, D_B and D_T are the Brownian diffusion coefficient and the thermophoresis diffusion coefficient, D_S is the solutal diffusivity, D_{TC} and D_{CT} are the Dufour and Soret type diffusivity, T_∞ is the free stream temperature, C_p is the specific heat at constant pressure, and g, k are the acceleration due to gravity, the thermal conductivity of the fluid, respectively. The last term on the right-hand side of the energy equation (3) and diffusion equation (4) signifies the diffusion-thermo effect and the thermal-diffusion effect, respectively.

The last term of right hand side of (2) represents the magnetic flux. The functional form of magnetic field is as $B_0(x)=2x^{\frac{m-1}{2}}$. The new set of dimensionless parameters defined to transform (1)-(5) and (6) into a set of non-dimensional equations are:

$$\begin{aligned} &\eta=y\sqrt{\frac{a(m+1)}{2\nu}}x^{\frac{m-1}{2}}, u=ax^m s'(\eta) \\ &v=-\sqrt{\frac{a(m+1)}{2\nu}}x^{\frac{m-1}{2}}\times\left(s(\eta)+\frac{m-1}{m+1}\eta s'(\eta)\right) \\ &\theta(\eta)=\frac{T-T_\infty}{T_w-T_\infty}, \gamma(\eta)=\frac{C-C_\infty}{C_w-C_\infty}, f(\eta)=\frac{\varphi-\varphi_\infty}{\varphi_w-\varphi_\infty} \end{aligned} \tag{7}$$

The continuity equation is automatically satisfied. The transformed momentum, energy and concentration equations together with the boundary conditions can be written as

$$s'''+ss''-\frac{2m}{m+1}s'^2-Ms'=0 \tag{8}$$

$$\frac{1}{\Pr}\theta''+s\theta'+Nb\theta' f'+Nt\theta'^2+Nd\gamma''=0 \tag{9}$$

$$\gamma''+Les\gamma'+Ld\theta''=0 \tag{10}$$

$$f''+Lnsf'+\frac{Nt}{Nb}\theta''=0 \tag{11}$$

And the corresponding boundary equations are transformed to

$$\begin{aligned} &s(0)=0, s'(0)=1, \theta(0)=1, \gamma(0)=1, f(0)=1, \ \text{at}\ \eta=0 \\ &s'(\infty)=0, \theta(\infty)\to 0, \gamma(\infty)\to 0, f(\infty)\to 0, \ \text{as}\ \eta\to\infty \end{aligned} \tag{12}$$

where primes denote differentiation with respect to η, and the

six parameters appearing in equations are defined as follows:

$$\Pr = \frac{\nu}{\alpha_m}, Ln = \frac{\nu}{D_B}, Le = \frac{\nu}{D_S}, Ld = \frac{D_{TC}(T_w - T_\infty)}{D_S(C_w - C_\infty)},$$

$$Nd = \frac{D_{TC}(C_w - C_\infty)}{\nu(T_w - T_\infty)}, M = \frac{8\sigma}{\rho_f a(m+1)}$$
$$Nb = \frac{(\rho c)_p D_B(\varphi_w - \varphi_\infty)}{(\rho c)_f \nu}, Nt = \frac{(\rho c)_p D_T(T_w - T_\infty)}{(\rho c)_f T_\infty \nu} \quad (13)$$

Pr, Ln, Le, Ld, m, M, Nd, Nb, and *Nt* denote the Prandtl number, the nanofluid Lewis number, regular Lewis number, Dufour-solutal Lewis number, the stretching parameter, the magnetic parameter, modified-Dufour parameter, the Brownian motion parameter, and the thermophoresis parameter, respectively.

III. Numerical Implementation: Finite Element Method

The finite element method (FEM) is a computer-based numerical method, which is used for solving various practical engineering problems that occur in many fields such as, in heat transfer, fluid mechanics [15], chemical processing [24], rigid body dynamics [25], solid mechanics [26] and so on. It is one the most powerful method in its application to real-world problems that involve complicated physics, geometry, and/or boundary conditions. As the name suggests, the basic concept lies in dividing the whole domain into smaller elements of finite dimensions. The governing differential equations are solved by transforming them into a matrix equation.

The given domain is viewed as a collection of subdomains, and over each subdomain the governing equation is approximated by any of the traditional variational methods. The reason behind finding approximate solution on the subdomains is that it is easier to represent a complicated function as a collection of simple polynomials. The essential step is to assume the piecewise continuous function for obtaining the solution. We have a set of simultaneous partial differential equations, given in (8)-(11), with (12) representing the boundary conditions. For the solution of these equations, assume that

$$s' = h \quad (14)$$

After substituting this, the system of (8)-(11) is reduced to

$$h'' + sh' - \frac{2m}{m+1}h^2 - Mh = 0 \quad (15)$$

$$\frac{1}{\Pr}\theta'' + s\theta' + Nb\theta' f' + Nt\theta'^2 + Nd\gamma'' = 0 \quad (16)$$

$$\gamma'' + Les\gamma' + Ld\theta'' = 0 \quad (17)$$

$$f'' + Lnsf' + \frac{Nt}{Nb}\theta'' = 0 \quad (18)$$

and the corresponding boundary conditions are as follows

$$s(0) = 0, h(0) = 1, \theta(0) = 1, \gamma(0) = 1, f(0) = 1, \text{ at } \eta = 0$$
$$h(\infty) = 0, \theta(\infty) \to 0, \gamma(\infty) \to 0, f(\infty) \to 0, \text{ as } \eta \to \infty \quad (19)$$

The weighted residual formulation of the given differential equations over the typical linear element denoted by Ωe having coordinates (ηe, ηe+1) is given by

$$\int_{\eta_e}^{\eta_{e+1}} W_1\{s' - h\}\, d\eta = 0$$
$$\int_{\eta_e}^{\eta_{e+1}} W_2\left\{h'' + sh' - \frac{2m}{m+1}h^2 - Mh\right\} d\eta = 0$$
$$\int_{\eta_e}^{\eta_{e+1}} W_3\left\{\frac{1}{\Pr}\theta'' + s\theta' + Nb\theta' f' + Nt\theta'^2 + Nd\gamma''\right\} d\eta = 0$$

$$\int_{\eta_e}^{\eta_{e+1}} W_4\{\gamma'' + Les\gamma' + Ld\theta''\} d\eta = 0$$
$$\int_{\eta_e}^{\eta_{e+1}} W_5\left\{f'' + Lnsf' + \frac{Nt}{Nb}\theta''\right\} d\eta = 0 \quad (20)$$

where W_1, W_2, W_3, W_4, and W_5 are arbitrary test functions. They can be considered as functions in s, h, θ, γ, and f, respectively.

In our computation, the shape functions for a typical element are taken as quadratic element. The finite element model thus formed is given by

$$\begin{bmatrix} [K^{11}] & [K^{12}] & [K^{13}] & [K^{14}] & [K^{15}] \\ [K^{21}] & [K^{22}] & [K^{23}] & [K^{24}] & [K^{25}] \\ [K^{31}] & [K^{32}] & [K^{33}] & [K^{34}] & [K^{35}] \\ [K^{41}] & [K^{42}] & [K^{43}] & [K^{44}] & [K^{45}] \\ [K^{51}] & [K^{52}] & [K^{53}] & [K^{54}] & [K^{55}] \end{bmatrix} \begin{bmatrix} s \\ h \\ \theta \\ \gamma \\ f \end{bmatrix} = \begin{bmatrix} \{b^1\} \\ \{b^2\} \\ \{b^3\} \\ \{b^4\} \\ \{b^5\} \end{bmatrix} \quad (21)$$

where $[K_{mn}]$ and $[b_m]$ (m, n=1,2,3,4,5) are defined as:

$$K_{ij}^{11}=\int_{\eta_e}^{\eta_{e+1}}\psi_i\frac{\partial\psi_j}{\partial\eta}d\eta, K_{ij}^{12}=-\int_{\eta_e}^{\eta_{e+1}}\psi_i\psi_j d\eta, K_{ij}^{13}=K_{ij}^{14}=K_{ij}^{15}=0$$
$$K_{ij}^{21}=K_{ij}^{23}=K_{ij}^{24}=K_{ij}^{25}=0$$

$$K_{ij}^{22}=-\int_{\eta_e}^{\eta_{e+1}}\frac{\partial\psi_i}{\partial\eta}\frac{\partial\psi_j}{\partial\eta}d\eta+\int_{\eta_e}^{\eta_{e+1}}\psi_i\bar{s}\frac{\partial\psi_j}{\partial\eta}d\eta-\frac{2m}{m+1}\int_{\eta_e}^{\eta_{e+1}}\psi_i\bar{h}\psi_j d\eta \quad -M\int_{\eta_e}^{\eta_{e+1}}\psi_i\psi_j d\eta$$

$$K_{ij}^{31}=K_{ij}^{32}=K_{ij}^{35}=0, K_{ij}^{34}=-Nd\int_{\eta_e}^{\eta_{e+1}}\frac{\partial\psi_i}{\partial\eta}\frac{\partial\psi_j}{\partial\eta}d\eta$$

$$K_{ij}^{33}=-\frac{1}{\mathrm{Pr}}\int_{\eta_e}^{\eta_{e+1}}\frac{\partial\psi_i}{\partial\eta}\frac{\partial\psi_j}{\partial\eta}d\eta+\int_{\eta_e}^{\eta_{e+1}}\psi_i\bar{s}\frac{\partial\psi_j}{\partial\eta}d\eta+Nb\int_{\eta_e}^{\eta_{e+1}}\psi_i\overline{f'}\frac{\partial\psi_j}{\partial\eta}d\eta$$
$$+Nt\int_{\eta_e}^{\eta_{e+1}}\psi_i\overline{\theta'}\frac{\partial\psi_j}{\partial\eta}d\eta$$

$$K_{ij}^{51}=K_{ij}^{52}=K_{ij}^{54}=0, K_{ij}^{53}=-\frac{Nt}{Nb}\int_{\eta_e}^{\eta_{e+1}}\frac{\partial\psi_i}{\partial\eta}\frac{\partial\psi_j}{\partial\eta}d\eta,$$

$$K_{ij}^{55}=-\int_{\eta_e}^{\eta_{e+1}}\frac{\partial\psi_i}{\partial\eta}\frac{\partial\psi_j}{\partial\eta}d\eta+Ln\int_{\eta_e}^{\eta_{e+1}}\psi_i\bar{s}\frac{\partial\psi_j}{\partial\eta}d\eta$$

$$K_{ij}^{41}=K_{ij}^{42}=K_{ij}^{45}=0, K_{ij}^{43}=-Ld\int_{\eta_e}^{\eta_{e+1}}\frac{\partial\psi_i}{\partial\eta}\frac{\partial\psi_j}{\partial\eta}d\eta,$$
$$K_{ij}^{44}=-\int_{\eta_e}^{\eta_{e+1}}\frac{\partial\psi_i}{\partial\eta}\frac{\partial\psi_j}{\partial\eta}d\eta+Le\int_{\eta_e}^{\eta_{e+1}}\psi_i\bar{s}\frac{\partial\psi_j}{\partial\eta}d\eta \qquad (22)$$

where

$$\bar{s}=\sum_{i=1}^{3}s_i\psi_i, \bar{s}'=\sum_{i=1}^{3}\bar{s}_i\frac{\partial\psi_i}{\partial\eta}, \bar{h}=\sum_{i=1}^{3}h_i\psi_i, \bar{h}'=\sum_{i=1}^{3}\bar{h}_i\frac{\partial\psi_i}{\partial\eta}$$
$$\bar{\theta}'=\sum_{i=1}^{3}\bar{\theta}_i\frac{\partial\psi_i}{\partial\eta}, \bar{\gamma}=\sum_{i=1}^{3}\gamma_i\psi_i, \bar{\gamma}'=\sum_{i=1}^{3}\bar{\gamma}_i\frac{\partial\psi_i}{\partial\eta}, \bar{f}'=\sum_{i=1}^{3}\bar{f}_i\frac{\partial\psi_i}{\partial\eta} \qquad (23)$$

For quadratic element case, the entire flow domain is divided into a set of 5000 quadratic elements. As every element is three-noded; therefore, the total number of nodes in domain are 10,001, and hence, a system of 50,005 nonlinear equations are obtained. An iterative scheme must be used to solve the system of equations. Gauss elimination method is used to solve the system while maintaining the accuracy of 0.00002. The relative difference between the current and present iterations is used as the convergence criterion. The integrations are solved by using the Gaussian quadrature method. MATLAB is used for executing the code of the algorithm. Multiple Regression Estimates (MRE) can be used for the comparison of various parameters namely, Nur, Shr, and Shrn. This is proposed in the next paper.

IV. Results and Discussions

To provide a physical insight into problem, numerical computations have been conducted for different values of

parameters that describe flow characteristics. The results are presented both in tabular form and graphically. The system of non-linear ordinary differential equations together with the boundary conditions are numerically solved by using FEM.

An extensive mesh testing procedure is conducted to suitably guess the value of n_∞ (length of domain), ensuring the grid independence solution of given boundary value problem. The region of integration η is considered from 0 to η_∞= 10, where η_∞ corresponds to η→∞ which lies well outside the momentum and thermal boundary layer (Table I).

The numerical values of reduced Nusselt number Nur, reduced local Sherwood number Shr and reduced nanofluid Sherwood number Shrn is presented in Table II.

From Table II, it can be observed that the magnitude of heat, regular and nano mass transfer rate is decreasing with the presence of magnetic parameter M for all values of Prandtl number Pr and Lewis number Ln. It is interesting to note that with the nanofluid Lewis number does not follow the same trend. With the increase in Ln, heat transfer rate decreases while the regular and nano fluid mass transfer rate increase.

The profiles of all the functions decrease monotonically with an increase in η. As η→∞, which represents the characteristic of boundary layer flow, the value reaches to zero asymptotically. Figs. 1-4 illustrate the effect of magnetic parameter M on velocity distribution s'(η) temperature profile θ(η), solutal concentration γ(η), and nanoparticle concentration f(η) through the boundary layer regime.

TABLE I
CALCULATION OF *NUR*, *SHR* AND *SHRN* WHEN $N_B=N_T=0.5$, $N_D=0.2$, $L_D=0.1$, $L_N=L_E=P_R=2.0$, $M=2$, $M=2$

Step size	Nur	Nur	Nur	Shr	Shr	Shr	Shrn	Shrn	Shrn
	η_∞= 8	η_∞= 10	η_∞= 12	η_∞= 8	η_∞= 10	η_∞= 12	η_∞= 8	η_∞= 10	η_∞= 12
0.2	0.22340	0.22355	0.22358	0.79974	0.79961	0.79968	0.71123	0.71007	0.71014
0.1	0.21790	0.21806	0.21812	0.80318	0.80305	0.80309	0.71945	0.71829	0.71829
0.04	0.21469	0.21485	0.21489	0.80433	0.80420	0.80425	0.72344	0.72228	0.72229
0.02	0.21364	0.21379	0.21385	0.80456	0.80443	0.80448	0.72461	0.72345	0.72349
0.01	0.21311	0.21327	0.21332	0.80464	0.80451	0.80457	0.72516	0.72400	0.72406
0.005	0.21285	0.21301	0.21308	0.80467	0.80454	0.80458	0.72543	0.72426	0.72429
0.002	0.21178	0.21285	0.21285	0.80498	0.80467	0.80456	0.72597	0.72442	0.72442

TABLE II
VARIATIONS IN *NUR*, *SHR* AND *SHRN* WITH *PR* AND *LN* WITH *M=0,2* WHEN $N_B=N_T=0.5$, $N_D=0.2$, $L_D=0.1$, $L_E=2.0$, $M=0.2$

Pr	Ln	Nur	Nur	Shr	Shr	Shrn	Shrn
		M=0	M=2	M=0	M=2	M=0	M=2
0.7	5	0.23493	0.16069	0.93820	0.76778	1.57195	1.38186
	15	0.22901	0.15759	0.93926	0.76833	2.92396	2.72508
	25	0.22748	0.15688	0.93962	0.76852	3.83781	3.63819
2.0	5	0.20985	0.15513	0.94554	0.76881	1.65367	1.40920
	15	0.18376	0.13680	0.94925	0.77144	3.03136	2.78399
	25	0.17762	0.13295	0.95045	0.77226	3.95140	3.70638
5.0	5	0.05137	0.04313	0.96162	0.77991	1.80158	1.51497
	15	0.03262	0.02673	0.96518	0.78287	3.15331	2.87875
	25	0.03078	0.02559	0.99664	0.78385	4.06256	3.79633

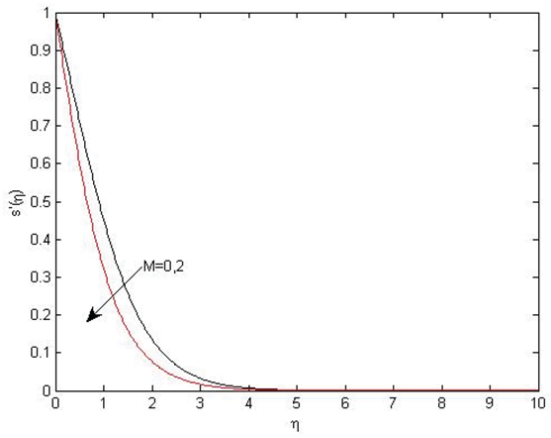

Fig. 1 Effect of magnetic parameter *M* on velocity distribution

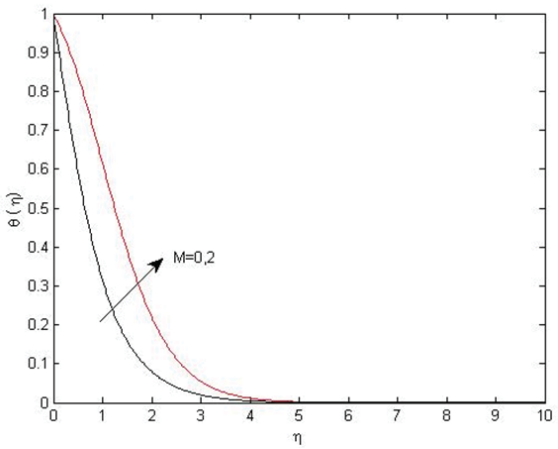

Fig. 2 Effect of magnetic parameter *M* on temperature distribution

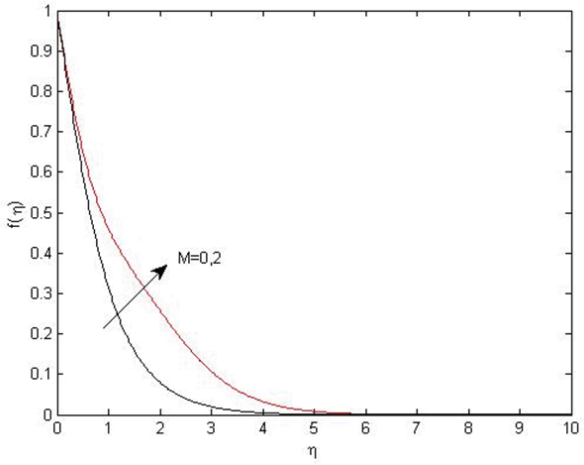

Fig. 3 Effect of magnetic parameter *M* on nanoparticle concentration

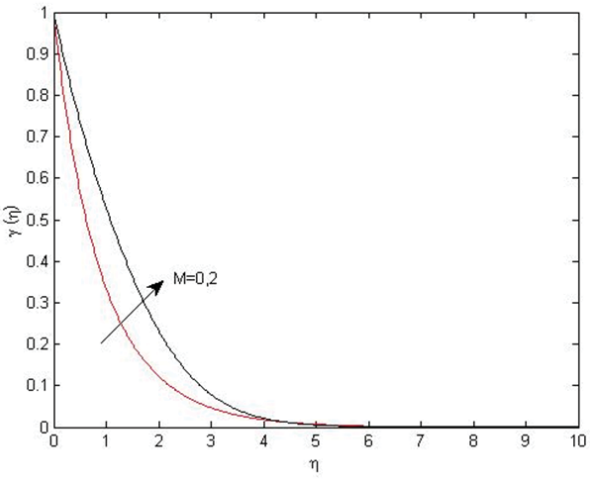

Fig. 4 Effect of magnetic parameter *M* on solutal concentration

With the presence of magnetic parameter M, the nanofluid velocity s'(η) tends to decrease. This is because an increase in Lorentz drag force opposes the fluid motion. On the other hand, it can be well determined from the table that the presence of magnetic parameter M leads to an increase in temperature profile θ(η), solutal concentration γ(η), and nano particle concentration f(η). This lowers the heat, regular, and nano mass transfer rate between the surface and the nanofluid. As name suggests, the values of Brownian motion parameter, Nb describe the strength of Brownian motion (random motion of particles). The effects of Brownian motion parameter Nb on the dimensionless heat, regular and nano mass transfer rate is shown in Figs. 5 (a)-(c). In case of M=0, the obtained profiles for Nur, Shr, and Shrn are in good agreement with results reported by Goyal and Bhargava [4].

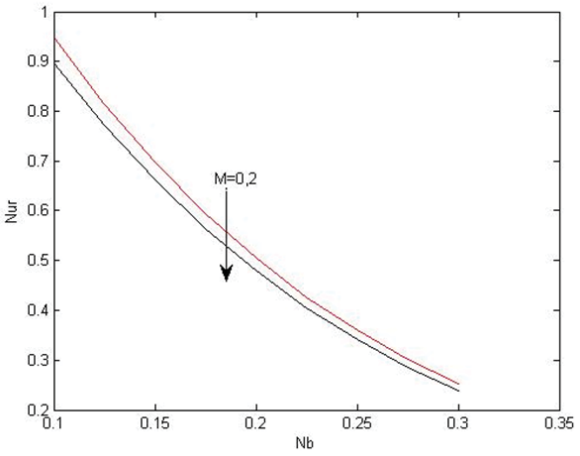

Fig. 5 (a) Effect of magnetic parameter *M* and Brownian motion parameter *Nb* on *Nur*

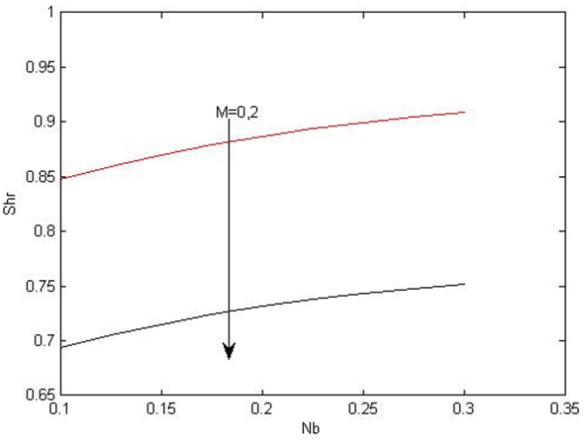

Fig. 5 (b) Effect of magnetic parameter *M* and Brownian motion parameter *Nb* on *Shr*

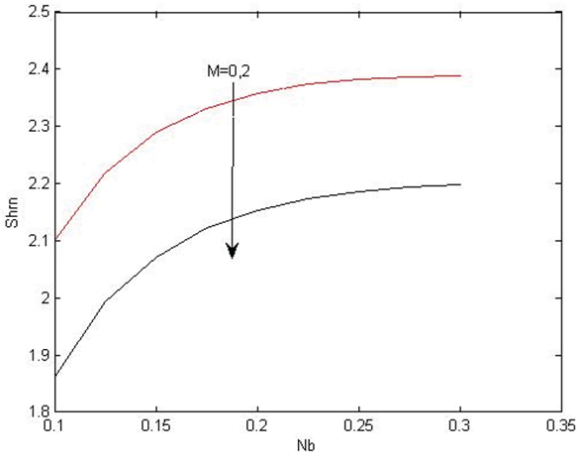

Fig. 5 (c) Effect of magnetic parameter *M* and Brownian motion parameter *Nb* on *Shrn*

With an increase in Nb, the thickness of thermal boundary

layer increases because of the increased Brownian motion of nanoparticles, whereas an increase in M leads to an increase in Lorentz drag force opposing the fluid motion. The combined effect of increase of both the parameters causes the temperature to increase, thus reducing the effective heat transfer (Fig 5 (a)). Figs. 5 (b) and (c) show the effect of Brownian motion along with the magnetic parameter on regular and nano mass transfer rate, respectively. With an increase in Nb, the increased random motion of particles serves to warm the boundary layer leading to the effective movement of nanoparticles from the wall of the stretching sheet to the inactive fluid. This intensifies the particle deposition away from the fluid, thereby justifying for the reduced concentration magnitudes ($\gamma(\eta)$and $f(\eta)$) and an increase in the regular mass transfer rate Shr and nano mass transfer rate Shrn.

The diffusion of particles under the effect of a temperature gradient is termed as thermophoresis. The thermophoresis parameter Nt is used to gauge this effect. Figs. 6 (a)-(c) show the effects of thermophoresis parameter Nt on the dimensionless heat, regular and nano mass transfer rate. Fig. 6 (a) shows the effect of thermophoresis parameter along with the magnetic parameter on heat transfer rate Nur. The thermophoretic force generated by the temperature gradient creates a fast flow away from the stretching surface. The simultaneous increase of both Nt and M causes an increase in heat transfer and consequently decreases the heat transfer rate Nur.

The thermophoretic effect Nt on regular and nano mass transfer rate can be observed in Fig. 6 (b) and (c). A decrease in magnetic parameter M supports the fluid flow motion because of the decrease in Lorentz drag force, causing an increase in mass flux.

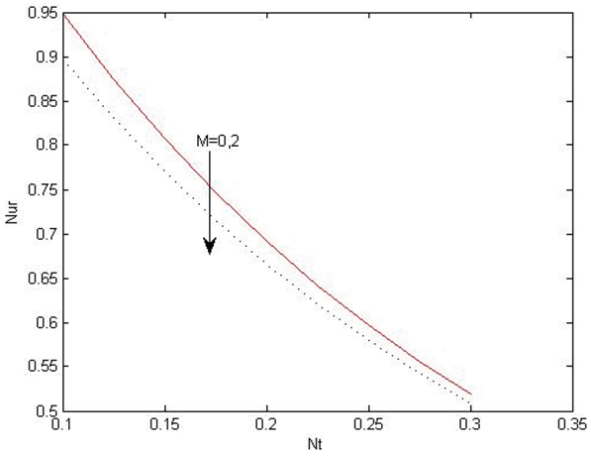

Fig. 6 (a) Effect of magnetic parameter *M* and Thermophoresis parameter *Nt* on *Nur*

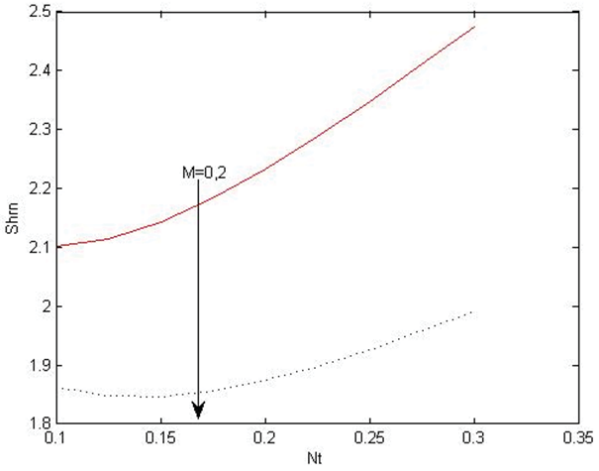

Fig. 6 (b) Effect of magnetic parameter *M* and Thermophoresis parameter *Nt* on *Shr*

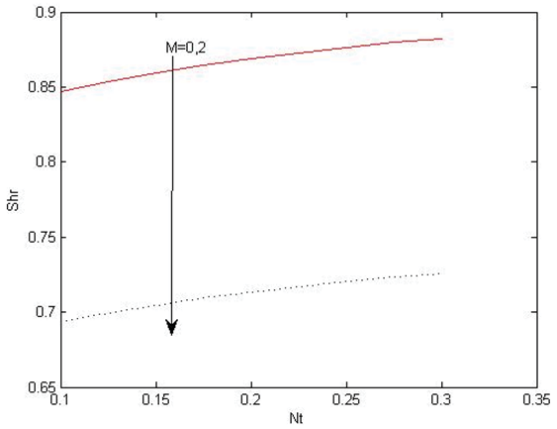

Fig. 6 (c) Effect of magnetic parameter *M* and Thermophoresis parameter *Nt* on *Shrn*

V. Conclusion

In the present paper, we have studied the boundary layer flow resulting from non-linear stretching of sheet embedded in a nanofluid, incorporating the effects of thermophoresis and Brownian motion along with variable magnetic field. The results can be summarized as follows:

1. Increasing the value of the magnetic parameter M decreases the momentum boundary layer thickness and increases the thermal, solutal and nano-mass volume fraction boundary layer thickness. An external magnetic fluid gives rise to magnetic body force (i.e. Lorentz drag force) opposing the fluid motion. By adjusting the external magnetic field, the heat transfer can be controlled. Recent development of "smart" cooling devices is based on this idea.
2. With the increasing value of Brownian motion parameter Nb and thermophoresis parameter Nt, the local heat transfer rate and local solutal and nano mass concentration decrease for an increase in the value of

magnetic parameter M. As different combinations of nanoparticles and base fluids have different values for these parameters (i.e. Nb and Nt), thus having different heat transfer rates. This idea can be used for customizing the heat transfer in stretching sheet problems.

3. With an increase in nanofluid Lewis number Ln, heat transfer rate decreases while the regular and nano fluid and mass transfer rate increases. Ln defines the ration of thermal diffusivity to mass diffusivity. It is used to characterize fluid flow when there is simultaneous heat and mass transfer by convection. With an increase in Ln, the Brownian diffusion decreases, hence forcing the concentration to decrease.
4. The magnitude of heat, regular, and nano mass transfer rates decreases with the increase in the magnetic parameter M because of an increase in Lorentz drag force.

ACKNOWLEDGMENT

Rangoli Goyal would like to thank Department of Science and Technology, Government of India, for its financial support through the award of a research grant. The second author RB proposes acknowledgement to DST SERB for her project.

REFERENCES

[1] Bachok N, Ishak A, Pop I (2012) Unsteady boundary layer flow and heat transfer of a nanofluid over a permeable stretching/shrinking sheet. Int. J. Heat Mass Transf. 55, 2102-2109.
[2] Buongiorno J. (2006) Convective transport in nanofluids. Jounal of Heat Transfer 128(3):240-250.
[3] Cortell R (2011) Heat and fluid flow due to non-linearly stretching surfaces, Appl Math Comput 217(19):7564-7572.
[4] Goyal M., Bhargava R., (2014) Numerical study of thermodiffusion effects on boundary layer flow of nanofluids over a power law stretching sheet, Microfluid Nanofluid, 17:591-604.
[5] Hamad MAA, Ferdows M (2012) Similarity solutions to viscous flow and heat transfer of nanofluid over non linearly stretching sheet, Appl. Math. Mech. 33, 923-930.
[6] Kechil S.A., Hashim I. (2008) Series solution of flow over nonlinearly stretching sheet with chemical reaction and magnetic field, Phys. Lett. A, 372, pp. 2258-2263.
[7] Khan WA, Aziz A (2011) Double diffusive natural convective boundary layer flow in a porous medium saturated with a nanofluid over a vertical plate: prescribed surface heat, solute and nanoparticle fluxes. Int. J. Therm. Sci. 50, 2154-2160.
[8] Kumaran, V., Ramanaiah, G. (1996) A note on the flow over a stretching sheet. ActaMechanica 116 (1-4), 229-233.
[9] Kuznetsov A, Nield D (2011) Double-diffusive natural convective boundary-layer flow of a nanofluid past a vertical plate. Int. J. Therm. Sci. 50(5):712-717.
[10] Makinde OD, Aziz A (2011) Boundary layer flow of a nanofluid past a stretching sheet with a convective boundary condition, Int. J. Therm. Sci. 50, 1326-1332.
[11] Matin MH, Dehsara M, Abbassi A (2012) Mixed convection MHD flow of nanofluid over a non-linear stretching sheet with effects of viscous dissipation and variable magnetic field, Mechanika Vol. 18(4), 415-423.
[12] Narayana M, Sibanda P (2012) Laminar flow of a nanoliquid film over an unsteady stretching sheet, Int. J. Heat Mass Transf. 55, 7552-7560.
[13] Nkurikiyimfura I, Wang Y, Pan Z (2013) Heat transfer enhancement by magnetic nanofluids - A review, Renewable and Sustainable Energy Reviews 21, 548-561.
[14] Odenbach S. (2004) Recent progress in magnetic fluid research. Journal of Physics: Condensed Matter 16: R1135-50.
[15] Reddy JN (1985) An introduction to the finite element method. McGraw-Hill Book Co, New York.
[16] Sakiadis BC. (1961) Boundary layer behaviour on continuous moving solid surfaces, I. Boundary layer equations for two-dimensional and axis-symmetric flow, II. Boundary layer on a continuous flat surface, III. Boundary layer on a continuous cylindrical surface. Am InstChemEng J; 7:26-8. 221-225, 467-472.
[17] Vajravelu K. (2001) Viscous flow over a nonlinearly stretching sheet, Applied Mathematics and Computation, vol. 124, no. 3, pp. 281-288.
[18] Vajravelu K., Prasad KV, Ng C (2013) Unsteady convective boundary layer flow of a viscous fluid at a vertical surface with variable fluid properties, Nonlinear analysis: Real world applications 14, 455-464.
[19] Masuda H, Ebata A, Teramae K, Hishinuma N (1993) Alteration of thermal conductivity and viscosity of liquid by dispersing ultrafine particles. NetsuBussei 7(4):227-233.
[20] Choi SUS, Zhang ZG, Yu W, Lockwood FE, Grulke EA (2001) Anomalous thermal conductivity enhancement in nanotube suspensions. ApplPhysLett 79(14):2252-2254.
[21] Choi SUS, Eastman JA (1995) Enhancing thermal conductivity of fluids with nanoparticles in developments and applications of non-newtonian flows, ASME FED-vol. 231/MD-vol. 66:99-105.
[22] Crane, L.J., (1970) Flow past a stretching plate, Volume 21, Issue 4, pp 645-647.
[23] Ziabakhsh Z., G. Domairry, H. Bararnia and H. Babazadeh (2010), Analytical solution of flow and diffusion of chemically reactive species over a non-linearly stretching sheet immersed in a porous medium. Journal of the Taiwan Institute of Chemical Engineers, vol. 14, 22-28.
[24] Lin YY, Lo SP (2003) Finite element modelling for chemical mechanical polishing process under different back pressures. J Mater Process Technol 140(1-3):646-652
[25] Dettmer W, Peric D (2006) A computational framework for fluid-rigidbody interaction: finite element formulation and applications. Comput Methods ApplMechEng 195(13-16):1633-1666.
[26] Hansbo A, Hansbo P (2004) A finite element method for the simulation of strong and weak discontinuities in solid mechanics. Comput Methods ApplMechEng 193(33-35):3523-3540.